

NON-LINEAR IMAGE PROCESSING[†]

P. R. Bell, R. S. Dillon,* and M. R. Bell**
Medical Instrumentation Group
Oak Ridge National Laboratory

ABSTRACT

Processing of nuclear medicine images is generally performed by essentially linear methods with the non-negativity condition being applied as the only non-linear process. The various methods used: matrix methods in signal space and Fourier or Hadamard transforms in frequency or sequency space are essentially equivalent. Further improvement in images can be obtained by the use of inherently non-linear methods. The recent development of an approximation to a least-difference method (as opposed to a least-square method) (1) has led to an appreciation of the effects of data bounding and to the development of a more powerful process. Data bounding (modification of statistically improbable data values) is an inherently non-linear method with considerable promise. Strong bounding depending on two-dimensional least-squares fitting yields a reduction of mottling (buttermilk effect) not attainable with linear processes. A pre-bounding process removing very bad points is used to protect the strong bounding process from incorrectly modifying data points due to the weight of an extreme but yet unbounded point as the fitting area approaches it.

NOTICE
This report was prepared as an account of work sponsored by the United States Government. Neither the United States nor the United States Energy Research and Development Administration, nor any of their employees, nor any of their contractors, subcontractors, or their employees, makes any warranty, express or implied, or assumes any legal liability or responsibility for the accuracy, completeness or usefulness of any information, apparatus, product or process disclosed, or represents that its use would not infringe privately owned rights.

CONFIDENTIAL

[†]Work performed by Union Carbide Corporation, Nuclear Division, for the U. S. Energy Research and Development Administration under U. S. Government Contract W-7405-eng-26.

* Computer Sciences Division, Union Carbide Corporation, Nuclear Division, Oak Ridge, Tennessee.

** UCC-ND Consultant.

By acceptance of this article, the publisher or recipient acknowledges the right of the U. S. Government to retain a nonexclusive, royalty-free license in and to any copyright covering the article.

NON-LINEAR IMAGE PROCESSING

P. R. Bell, R. S. Dillon, and M. R. Bell

Linear image smoothing methods are often applied to data with low statistical weight to improve the quality of the image so that details of the imaged structure will be more apparent to the observer. One effect of such smoothing, although details may be more visible, is the lumpy or "buttermilk" appearance of regions of the image that were expected to be smooth. This effect is produced by the removal of higher frequency noise components that had concealed these lower frequency components of the statistical fluctuation of the data. In essence, a data point that is so high or low as to have low probability will likely be surrounded by points closer to the mean and will appear in the processed image as a positive or negative delta function response of the processing function superimposed on a mildly fluctuating background. If the processing function has been chosen to fit the resolution of the imaging system for optimum signal/noise ratios, these noise lumps will resemble the image of a point source. Linear methods, whether in the signal or frequency domains, are powerless to suppress these fluctuation effects.

It was noted that data bounding, that is, the modification of data points of statistically improbably high or low values, had a noticeable beneficial effect upon the mottling or "buttermilk" effect in images with low counting rate. A recent article by Rempel (1) detailing an inherently non-linear procedure approximating a least-difference method demonstrated a strong beneficial effect in the smoothing of geophysical data. Data bounding is clearly a sort of black and white version of this method when applied using a least-squares fit against which to test the data points to be bounded.

Our bounding method performs a least-squares fit of a two-dimensional quadratic (or quartic) equation to a 7×7 (or 5×5) element array of the data at each point (2). The routine compares the data value with the fitted value $\pm 0.7, 1.0$, or 1.4 times the square root of the fitted value. If the data point lies outside the chosen range, it is replaced by the fitted value; otherwise it is left unchanged.

A 64×32 element field (2048 points) of Poisson distribution noise with $n = 5$ was prepared as a test object with a "detail," a 3×20 element bar of $n = 8$ noise. The FOCAL program used to produce this noise is given in Fig. 1. The random number generator used was the FRAN8 (DECUS FOCAL 8-150) not the standard FRAN FOCAL function which is not sufficiently random for this use. Figure 2 displays this raw noise field together with a Z-cut of the line through the long dimension of the signal bar. The background corresponds to a level of 45 counts/cm^2 in the usual 3-element/cm camera image while the signal bar corresponds to a $1 \text{ cm} \times 7 \text{ cm}$ area at 72 counts/cm^2 . The image was processed by multiple passes of various processing methods: 1) The usual 9-point (3×3) averaging, marked A4 in the image tags; 2) a 7×7 element Gaussian averager (Table 1) indicated as A5 in the tags; 3) a 7×7 element least-squares quadratic (Table 2) indicated as A2 in the tags. All these smoothers have a weight of 4 in the program so that the resulting processed data can display the

smoothing effect in integer form. The tag S2 corresponds to the least-squares fit A2 with a weight of 1, similarly for S4. The bounding processes are tagged B12 which is bounding to ± 0.7 standard deviations from the least-squares fit S2 and B22 means bounding to 1 standard deviation from fit S2.

Three passes of the 9-point smoothing are compared with one hard bounding and 3 passes of the least-squares quadratic smoothing in Fig. 3. Note the reduction of the magnitude of the "buttermilk" effect without a loss of signal contrast. Figure 4 displays histograms of a 15 x 20 element area on the right half of each image. The reduction of the spread of element values is evident. Figure 5 illustrates the performance of other processing combinations.

An area of 3 x 40 elements, half covering the signal bar and half covering the adjacent background area, is histogrammed in Fig. 6 to show the separation of the signal and noise for the raw data, the 9-point smoothing and the bounded and least-squares smoothed data.

Demonstration of processing on phantoms or synthetic data is well enough but it is necessary to show the effects on real patient images for a conclusive test. Figure 7 shows the application of the bounding and least-squares smoothing to a portion of a ^{67}Ga scan in comparison with the more conventional smoothing. The Z-cut shows the superior smoothing obtained with greater relief of detail above the surroundings.

References

- (1) Rempel, C. G.: "Nonlinear (Parabolic) Smoothing of Experimental Data," *Izv., Earth Physics*, No. 3, pp. 101-105 (1974).
- (2) Bell, M. R.: "A One and Two Dimensional Least Squares Smoothing and Edge-Sharpening Method for Image Processing," ORNL-TM-5222 (1976).

Figure 1. A FOCAL program to generate Poisson noise for any mean value n , not limited to integral values. The function FADC stores integer values in field 1. The FRAN function uses DECUS FOCAL 8-150 for good randomness.

```

01.05 A "N",N
01.10 S Y=1/FEXP(N)
01.20 F I=3,2047;D 2
01.30 Q

02.10 S X=1;S V=-1
02.20 S X=X*FABS(FRAN());S V=V+1
02.30 I (Y-X)2.2
02.40 S X=FADC(I,V)

```

TABLE 1

GAUSSIAN

(Blanks Represent Symmetric Entries)

.003	-	-	-	-
.013	.060	-	-	-
.022	.101	.162	-	-
-	-	-	-	-
-	-	-	-	-

TABLE 2

LEAST-SQUARES QUADRATIC

(Blanks Represent Symmetric Entries)

-7	-	-	-	-	-	-
-2	3	-	-	-	-	-
1	6	9	-	-	-	-
2	7	10	11	-	-	-
-	-	-	-	-	-	-
-	-	-	-	-	-	-
-	-	-	-	-	-	-

$\frac{1}{147}$



Figure 2. Random Poisson noise for $n = 5$ with a 3×20 element bar of $n = 8$ Poisson noise. The Z-cut passes through this bar. The lowest row of data points are ones.

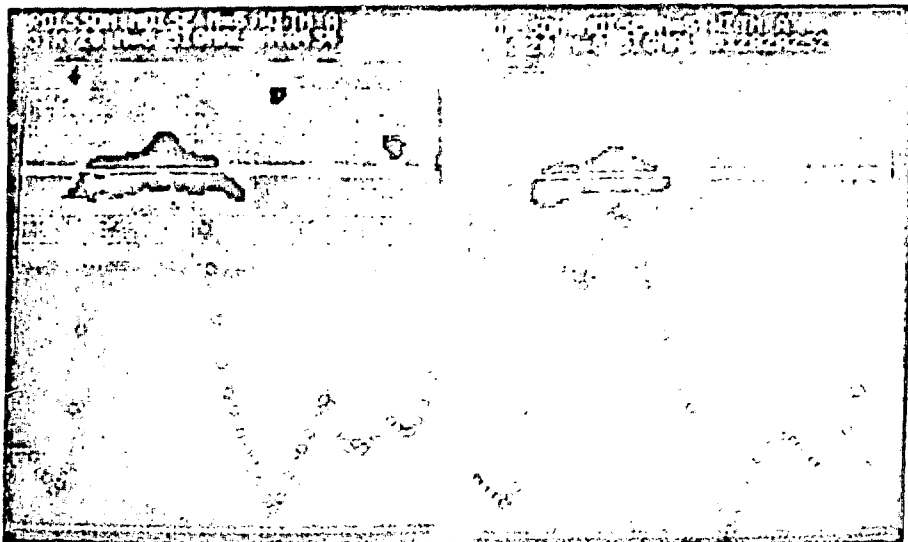


Figure 3. On the left is the noise processed by 3 passes of the 9-point smoother. A value was subtracted from every point of each image to reduce the lowest point of the noise fluctuation to zero. The right image and Z-cut are for the data after bounding to 0.7 SD and 3 passes of the two-dimensional quadratic least-squares fit. Note the reduced range of the fluctuations without loss of signal contrast. The display is a multicycle plot with a black component exceeding the lowest cycle

A4A4S4

B12A2A2S2

```

00
01
02XXXX
03XXXXXXXXXXXX
04XXXXXXXXXXXXXXXX
05XXXXXXXXXXXXXXXXXXXX
06XXXXXXXXXXXXXXXXXXXX
07XXXXXXXXXXXXXXXXXXXXXXXXXXXXXXXXXXXXXXXX
08XXXXXXXXXXXXXXXXXXXXXXXXXXXXXXXXXXXX
09XXXXXXXXXXXXXXXXXXXXXXXXXXXXXXXXXXXXXXXX
10XXXXXXXXXXXXXXXXXXXXXXXXXXXXXXXXXXXX
11XXXXXXXXXXXXXXXXXXXXXXXXXXXXXXXXXXXXXXXXXXXX
12XXXXXXXXXXXXXXXXXXXXXXXXXXXX
13XXXXXXXXXXXXXXXXXXXXXXXXXXXX
14XXXXXXXXXXXXXXXXXXXX
15XXXXX
16

```

```

00
01XXXX
02XXXXXXXX
03XXXXXXXXXXXXXXXX
04XXXXXXXXXXXXXXXXXXXX
05XXXXXXXXXXXXXXXXXXXX
06XXXXXXXXXXXXXXXXXXXX
07XXXXXXXXXXXXXXXXXXXXXXXXXXXXXXXXXXXX
08XXXXXXXXXXXXXXXXXXXXXXXXXXXXXXXXXXXXXXXXXXXX
09XXXXXXXXXXXXXXXXXXXXXXXXXXXXXXXXXXXXXXXXXXXX
10XXXXXXXXXXXXXXXXXXXXXXXXXXXXXXXXXXXX
11XXXXXXXXXXXXXXXXXXXX
12XXXXXX
13
14
15
16

```

Figure 4. 15 x 20 element histograms of the noise in the images of Fig. 3. Note the narrower and higher distribution for the bounded data.

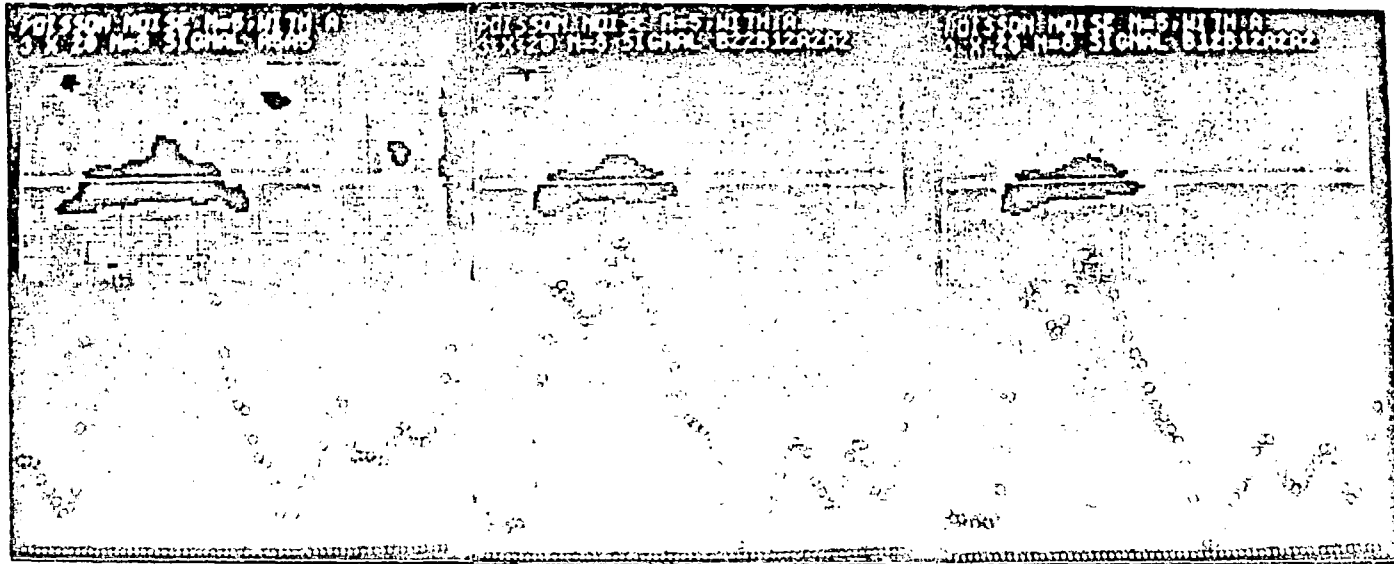


Figure 5. 3 different processing procedures of intermediate degree of fluctuation compared with those of Fig. 3.

RAW DATA

```

00
01XXXX
02XXXXXXXXXXXXXXXXXX
03XXXXXXXXXXXXXXXXXX
04XXXXXXXXXXXXXXXXXX
05XXXXXXXXXXXXXXXXXX
06XXXXXXXXXXXXXXXXXX
07XXXXXXXXXXXXXXXXXX
08XXXXXXXXXXXXXXXXXX
09XXXXXXXXXX
10XXXXXXXXXXXXXXXXXX
11XXXXXX
12XX
13XXXX
14XX
15XX
16
17
18
19
20
21
22
23
24
25
26
27
28
29
30
31

```

A4A4S4

```

00X
01XXXX
02XXXX
03XXXXX
04XXXX
05XXXXXXXXXX
06XXXXXXXXXX
07XXXXXXXXXX
08XXXX
09XXXXXXXXXX
10XX:
11XXXXXXXXXX
12XXX
13X
14XXX
15XX
16X
17XXX
18XX
19XX
20XX
21XXXXXX
22XX
23XXXXXXXXXX
24XXXXXXXXXX
25XXXXX
26XXXXX
27XXXXXXXXXXXXXXXXXX
28XXXXXXXXXX
29XXXXX
30XXXXXXXXXX
31XXXXXX

```

B12A2A2S2

```

00
01XX
02XXXXX
03XXXX
04XXXX
05XXXXXX
06:XXX
07XX
08XXXXXXXXXXXXXX
09XXXXXXXXXX
10XXXX,XXXXXX
11XXXXX
12X
13XXXX
14XX
15XXXX
16XX
17XX
18XX
19XX
20XXXX
21XXXXXXXXXXXXXX
22XXXXXXXXXXXXXX
23XXXXXX
24XXXXXXXXXX
25XXXXXX
26XXXXXXXXXXXX
27XXXXX
28XXXXXXXXXXXX
29XXXXX
30XX
31

```

SIGNAL PLUS NOISE

Figure 6. Histograms of an area half on and half off of the signal bar. The signal is not resolved in the raw data but is resolved in the others.

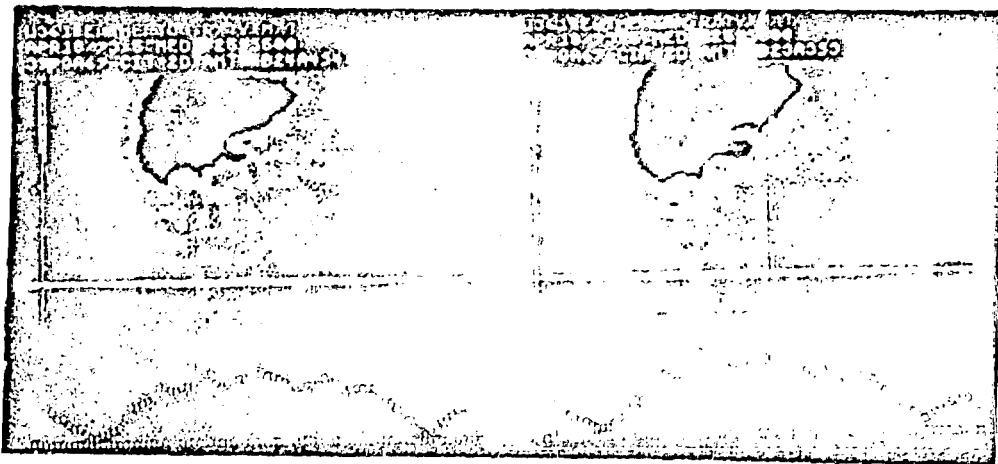


Figure 7. Two processes applied to part of a ^{67}Ga scan image. Note the better detail relief and reduction of noise lumpiness in the bounded and least-squares smoothed image on the right compared to the Gaussian bounded and smoothed image on the left.